

Co[HO<sub>2</sub>C(CH<sub>2</sub>)<sub>3</sub>NH(CH<sub>2</sub>PO<sub>3</sub>H)<sub>2</sub>]<sub>2</sub>: A New Canted AntiferromagnetBing-Ping Yang,<sup>†</sup> Andrey V. Prosvirin,<sup>‡</sup> Ya-Qin Guo,<sup>†</sup> and Jiang-Gao Mao<sup>\*,†</sup>

State Key Laboratory of Structural Chemistry, Fujian Institute of Research on the Structure of Matter, Chinese Academy of Sciences, Fuzhou, Fujian 350002, P. R. China Department of Chemistry, Texas A&amp;M University, P.O. Box 30012, College Station, Texas 77843-3255

Received July 8, 2007

A new cobalt(II) carboxylate–phosphonate, namely, Co[HO<sub>2</sub>C(CH<sub>2</sub>)<sub>3</sub>NH(CH<sub>2</sub>PO<sub>3</sub>H)<sub>2</sub>]<sub>2</sub>, with a layered architecture has been synthesized by hydrothermal reactions. The Co(II) ion in the title compound is octahedrally coordinated by six phosphonate oxygen atoms from four carboxylate phosphonate ligands. Neighboring CoO<sub>6</sub> octahedra are interconnected by phosphonate groups into a 2D layer with a 4,4-net topology. Adjacent layers are further cross-linked via hydrogen bonds between the noncoordinate carboxylate groups and noncoordinate phosphonate oxygens. The ac and dc magnetic susceptibility and magnetization measurements indicate that Co[HO<sub>2</sub>C(CH<sub>2</sub>)<sub>3</sub>NH(CH<sub>2</sub>PO<sub>3</sub>H)<sub>2</sub>]<sub>2</sub> is a canted antiferromagnet with  $T_c = 8.75$  K.

## Introduction

The chemistry of metal phosphonates has been an active research area in recent years due to its potential applications in the areas of catalysis, ion exchange, proton conductivity, intercalation chemistry, photochemistry, and magnetic materials chemistry.<sup>1,2</sup> In addition to a variety of open frameworks such as layered and pillared layered structures,<sup>1–10</sup> metal phosphonates can also form a variety of isolated

clusters especially in the presence of a suitable auxiliary ligand.<sup>11,12</sup> In order to design metal phosphonates with open frameworks, a variety of functional groups such as amino

\* Author to whom correspondence should be addressed. E-mail: mjg@fjirsm.ac.cn.

<sup>†</sup> Chinese Academy of Sciences.

<sup>‡</sup> Texas A&M University.

- (1) (a) Clearfield, A. Metal Phosphonate Chemistry. In *Progress in Inorganic Chemistry*; Karlin, K. D., Ed.; John Wiley & Sons: New York, 1998; Vol. 47, pp 371–510 (and references therein). (b) Mao, J.-G. *Coord. Chem. Rev.* **2007**, *251*, 1493. (c) Matczak-Jon, E.; Videnova-Adrabsinska, V. *Coord. Chem. Rev.* **2005**, *249*, 2458.
- (2) (a) Cheetham, A. K.; Ferey, G.; Loiseau, T. *Angew. Chem., Int. Ed.* **1999**, *38*, 3268. (b) Zhu, J.; Bu, X.; Feng, P.; Stucky, G. D. *J. Am. Chem. Soc.* **2000**, *122*, 11563. (c) Rao, C. N. R.; Natarajan, S.; Vaidhyanathan, R. *Angew. Chem., Int. Ed.* **2004**, *43*, 1466.
- (3) (a) Kong, D. Y.; Li, Y.; Xiang, O. Y.; Prosvirin, A. V.; Zhao, H. H.; Ross, J. H.; Dunbar, K. R.; Clearfield, A. *Chem. Mater.* **2004**, *16*, 3020. (b) Gomez-Alcantara, M. M.; Cabeza, A.; Martinez-Lara, M.; Aranda, M. A. G.; Suau, R.; Bhuvanesh, N.; Clearfield, A. *Inorg. Chem.* **2004**, *43*, 5283. (c) Kong, D. Y.; Clearfield, A. *Chem. Commun.* **2005**, 1005. (d) Kong, D. Y.; Medvedev, D. G.; Clearfield, A. *Inorg. Chem.* **2004**, *43*, 7308. (e) Kong, D.; Zon, J.; McBee, J.; Clearfield, A. *Inorg. Chem.* **2006**, *45*, 977.
- (4) (a) Bao, S. S.; Ma, L. F.; Wang, Y.; Fang, L.; Zhu, C. J.; Li, Y. Z.; Zheng, L. M. *Chem.—Eur. J.* **2007**, *13*, 2333. (b) Cao, D. K.; Xiao, J.; Tong, J. W.; Li, Y. Z.; Zheng, L. M. *Inorg. Chem.* **2007**, *46*, 428. (c) Liu, B.; Yin, P.; Yi, X. Y.; Gao, S.; Zheng, L. M. *Inorg. Chem.* **2006**, *45*, 4205. (d) Bao, S. S.; Chen, G. S.; Wang, Y.; Li, Y. Z.; Zheng, L. M.; Luo, Q. H. *Inorg. Chem.* **2006**, *45*, 1124. (e) Yin, P.; Gao, S.; Wang, Z. M.; Yan, C. H.; Zheng, L. M.; Xin, X. Q. *Inorg. Chem.* **2005**, *44*, 2761.

- (5) (a) Mao, J.-G.; Wang, Z.-K.; Clearfield, A. *Inorg. Chem.* **2002**, *41*, 6106. (b) Mao, J.-G.; Clearfield, A. *Inorg. Chem.* **2002**, *41*, 2319. (c) Song, J.-L.; Zhao, H.-H.; Mao, J.-G.; Dunbar, K. R. *Chem. Mater.* **2004**, *16*, 1884. (d) Song, J. L.; Mao, J.-G. *Chem.—Eur. J.* **2005**, *11*, 1417. (e) Yang, B. P.; Mao, J. G. *Inorg. Chem.* **2005**, *44*, 566. (f) Song, J. L.; Lei, C.; Mao, J. G. *Inorg. Chem.* **2004**, *43*, 5630.
- (6) (a) Stock, N.; Bein, T. *Angew. Chem., Int. Ed.* **2004**, *43*, 749. (b) Serre, C.; Stock, N.; Bein, T.; Ferey, G. *Inorg. Chem.* **2004**, *43*, 3159. (c) Forster, P. M.; Stock, N.; Cheetham, A. K. *Angew. Chem., Int. Ed.* **2005**, *44*, 7608. (d) Bauer, S.; Muller, H.; Bein, T.; Stock, N. *Inorg. Chem.* **2005**, *44*, 9464. (e) Serre, C.; Groves, J. A.; Lightfoot, P.; Slawin, A. M. Z.; Wright, P. A.; Stock, N.; Bein, T.; Haouas, M.; Taulelle, F.; Ferey, G. *Chem. Mater.* **2006**, *18*, 1451.
- (7) (a) Groves, J. A.; Miller, S. R.; Warrender, S. J.; Mellot-Draznieks, C.; Lightfoot, P.; Wright, P. A. *Chem. Commun.* **2006**, 3305. (b) Groves, J. A.; Wright, P. A.; Lightfoot, P. *Dalton Trans.* **2005**, 2007. (c) Devi, R. N.; Wormald, P.; Cox, P. A.; Wright, P. A. *Chem. Mater.* **2004**, *16*, 2229.
- (8) (a) Zhang, X. M.; Hou, J. J.; Zhang, W. X.; Chen, X. M. *Inorg. Chem.* **2006**, *45*, 8120. (b) Tsao, C. P.; Sheu, C. Y.; Nguyen, N.; Lii, K. H. *Inorg. Chem.* **2006**, *45*, 6361. (c) Burkholder, E.; Golub, V.; O'Connor, C. J.; Zubieta, J. *Inorg. Chem.* **2004**, *43*, 7014. (d) Lin, C. H.; Lii, K. H. *Inorg. Chem.* **2004**, *43*, 6403. (e) Murugavel, R.; Shanmugan, S. *Chem. Commun.* **2007**, 1257.
- (9) (a) Fredoueil, F.; Evain, M.; Massiot, D.; Bujoli-Doeuff, M.; Janvier, P.; Clearfield, A.; Bujoli, B. *J. Chem. Soc., Dalton Trans.* **2002**, 1508. (b) Rabu, P.; Janvier, P.; Bujoli, B. *J. Mater. Chem.* **1999**, *9*, 1323. (c) Drumel, S.; Janvier, P.; Bujoli-Doeuff, M.; Bujoli, B. *J. Mater. Chem.* **1996**, *6*, 1843.
- (10) (a) Distler, A. S.; Sevov, C. *Chem. Commun.* **1998**, 959. (b) Lohse, D. L.; Sevov, S. C. *Angew. Chem., Int. Ed.* **1997**, *36*, 1619. (c) Turner, A.; Jaffres, P. A.; MacLean, E. J.; Villemain, D.; McKee, V.; Hix, G. B. *Dalton Trans.* **2003**, 1314. (d) Hartman, S. J.; Todorov, E.; Cruz, C.; Sevov, S. C. *Chem. Commun.* **2000**, 1213. (e) Hix, G. B.; Wragg, D. S.; Wright, P. A.; Morris, R. E. *J. Chem. Soc., Dalton Trans.* **1998**, 3359.

acids, crown ethers, amino groups, and carboxylates have been attached to the phosphonate groups.<sup>3–10</sup> Furthermore, the introduction of a second ligand such as 4,4'-bipy or an oxalate anion has been used as an effective synthetic tool, since these molecules can act as pillars between neighboring layers or be grafted into the inorganic layer to form a new hybrid layered architecture.<sup>3–10</sup> Recently, a variety of nano-materials based on metal phosphonates have been prepared.<sup>13</sup>

The cobalt phosphonates typically display interesting magnetic properties, such as canted antiferromagnetism in 3D  $\text{Co}_3(\text{O}_3\text{PC}_2\text{H}_4\text{CO}_2)_2$ ,<sup>9b</sup>  $\{\text{K}_2[\text{CoO}_3\text{PCH}_2\text{N}(\text{CH}_2\text{CO}_2)_2]\}_6 \cdot x\text{H}_2\text{O}$ , and 1D  $[\text{NH}_3(\text{CH}_2)_5\text{NH}_3][\text{Co}_2(\text{hedpH})_2 \cdot 2\text{H}_2\text{O}]$ .<sup>14</sup> Of particular interest is the cobalt(II) aminodiphosphonate with single-chain-magnet behavior that was reported by our group recently.<sup>15</sup> The manner in which the carboxylate group is attached to the  $-\text{N}(\text{CH}_2\text{PO}_3\text{H}_2)$  aminodiphosphonate moiety and the reaction conditions have a dramatic effect on the structures and properties of the corresponding cobalt(II) phosphonates isolated. For example, the carboxylate-phosphonate ligand in  $\{\text{Co}[(\text{HO}_2\text{CCH}_2\text{N}(\text{CH}_2\text{PO}_3\text{H}_2))]_2(\text{H}_2\text{O})_2\}$  chelates tetradentately with a metal center to yield a discrete molecule,<sup>16a</sup> whereas in  $\{\text{Co}_3[(\text{O}_2\text{CCH}_2\text{N}(\text{CH}_2\text{PO}_3\text{H}_2))]_2 \cdot (\text{H}_2\text{O})_4(4,4'\text{-bipy})_2\} \cdot 11\text{H}_2\text{O}$ , two such chelating units are bridged by the third metal center into a trinuclear unit; these cluster units are further interconnected by 4,4'-bipy ligands into a layered structure.<sup>5c</sup> Studies show that, when the carboxylate group is separated by a rigid benzene ring from the  $-\text{N}(\text{CH}_2\text{PO}_3\text{H}_2)_2$  moiety, the system  $\text{Co}^{2+}/\text{HO}_2\text{C}-\text{C}_6\text{H}_4-\text{N}(\text{CH}_2\text{PO}_3\text{H}_2)_2/\text{NaOH}$  yields four different compounds depending on the pH value and the nature of the counteranion; the carboxylate groups in these compounds are not involved in metal coordination.<sup>16b</sup> When 4,4'-bipy was used as the second metal linker, a different cobalt(II) phosphonate with

a pillared layered structure was isolated in which the noncoordinated  $-\text{C}_6\text{H}_4-\text{COOH}$  groups occupy the tunnels in the 3D structure.<sup>16c</sup>

In order to obtain additional insight into the structures and magnetic properties of this class of compounds, *N,N*-bis-(phosphonomethyl)-amino-butyric acid ( $\text{H}_5\text{L} = \text{HO}_2\text{-C}(\text{CH}_2)_3\text{N}(\text{CH}_2\text{PO}_3\text{H}_2)_2$ ), in which the carboxylate group is well separated from the diphosphonate part by a flexible alkyl group, was selected in this study. Thus far, only layered Zr(IV) and layered Pb(II) compounds of this ligand have been structurally characterized.<sup>17</sup> Herein, we report the synthesis, crystal structure, and magnetic properties of a new layered cobalt(II) carboxylate-phosphonate, namely,  $\text{Co}[\text{HO}_2\text{C}(\text{CH}_2)_3\text{NH}(\text{CH}_2\text{PO}_3\text{H}_2)]_2$ .

## Experimental Section

**Materials and Physical Measurements.** The carboxylate phosphonate ligand, *N,N*-bis(phosphonomethyl)-amino-butyric acid ( $\text{H}_5\text{L} = \text{HO}_2\text{C}(\text{CH}_2)_3\text{N}(\text{CH}_2\text{PO}_3\text{H}_2)_2$ ), was synthesized by a Mannich-type reaction according to procedures described previously.<sup>17</sup> All other chemicals were used as received without further purification. Elemental analyses were performed on a German Elementary Vario EL III instrument. The FT-IR spectrum was recorded in the range of 400–4000  $\text{cm}^{-1}$  on a Nicolet Magna 750 FT-IR spectrometer using a KBr pellet. Magnetic susceptibility measurements were carried out on a Quantum Design SQUID magnetometer, MPMS-XL. The raw data were corrected for the susceptibility of the container and the diamagnetic contributions of the sample using Pascal's constants. Thermogravimetric analysis (TGA) was performed on a NETZSCH STA 449C unit, at a heating rate of 15  $^\circ\text{C}/\text{min}$  under a nitrogen atmosphere.

**Synthesis of  $\text{Co}[\text{HO}_2\text{C}(\text{CH}_2)_3\text{NH}(\text{CH}_2\text{PO}_3\text{H}_2)]_2$ .** A mixture of cobalt(II) acetate (0.5 mmol),  $\text{HO}_2\text{C}(\text{CH}_2)_3\text{N}(\text{CH}_2\text{PO}_3\text{H}_2)_2$  (0.5 mmol), acetic acid (2 mL), and distilled water (8 mL) was placed into a Parr Teflon-lined autoclave (23 mL) and heated at 165  $^\circ\text{C}$  for 4 days; then, it was cooled to room temperature at a rate of 3  $^\circ\text{C}/\text{hr}$ . The initial and final pH values were close to 2.0. Pink needle-shaped crystals of the title compound were collected in a ca. 80% yield on the basis of Co. It was found that a low cooling rate is essential for the growth of high-quality crystals, as rapid cooling only led to pink powders. Elem anal. for  $\text{C}_{12}\text{H}_{28}\text{CoN}_2\text{O}_{16}\text{P}_4$ : C, 22.37; H, 4.25; N, 4.56. Calcd.: C, 22.55; H, 4.42; N, 4.38%. IR data ( $\text{cm}^{-1}$ ): 3130 (br), 1660 (m), 1403 (s), 1311 (m), 1246 (m), 1145 (m), 1084 (m), 1044 (m), 942 (m), 817 (m), 771 (m), 573 (m), 479 (m).

**X-Ray Crystallography.** A single crystal with dimensions of  $0.20 \times 0.15 \times 0.03 \text{ mm}^3$  was mounted on a Rigaku Mercury CCD diffractometer equipped with graphite-monochromated Mo K $\alpha$  radiation ( $\lambda = 0.71073 \text{ \AA}$ ). Intensity data were collected by the narrow frame method with  $0.3^\circ$  per frame in  $\omega$  at 293 K. A total of 2455 independent reflections were collected, among which 2127 reflections with  $I > 2.0\sigma(I)$  were considered observed. Empirical absorption corrections based on the multiscan method were applied.<sup>18</sup> The structure was solved by the direct methods and refined by full-matrix least-squares fitting based on  $F^2$  by SHELXS 97.<sup>18</sup>

- (11) (a) Baskar, V.; Shanmugan, M.; Sanudo, E. C.; Shanmugan, M.; Collison, D.; McInnes, E. J. L.; Wei, Q.; Winpenny, R. E. P. *Chem. Commun.* **2007**, 37. (b) Shanmugan, M.; Chastanet, G.; Mallah, T.; Sessoli, R.; Teat, S. J.; Timco, G. A.; Winpenny, R. E. P. *Chem.—Eur. J.* **2006**, *12*, 8777. (c) Konar, S.; Bhuvanesh, N.; Clearfield, A. J. *Am. Chem. Soc.* **2006**, *128*, 9604. (d) Langley, S. J.; Helliwell, M.; Sessoli, R.; Rosa, P.; Wernsdorfer, W.; Winpenny, R. E. P. *Chem. Commun.* **2005**, 5029. (e) Maheswaran, S.; Chastanet, G.; Teat, S. J.; Mallah, T.; Sessoli, R.; Wernsdorfer, W.; Winpenny, R. E. P. *Angew. Chem., Int. Ed.* **2005**, *44*, 5044. (f) Langley, S.; Helliwell, M.; Raftery, J.; Tollis, E. L.; Winpenny, R. E. P. *Chem. Commun.* **2004**, 142.
- (12) (a) Du, Z. Y.; Xu, H. B.; Mao, J.-G. *Inorg. Chem.* **2006**, *45*, 9780. (b) Du, Z. Y.; Xu, H. B.; Mao, J.-G. *Inorg. Chem.* **2006**, *45*, 6424. (c) Yao, H. C.; Wang, J. J.; Ma, Y. S.; Waldmann, O.; Du, W. X.; Song, Y.; Li, Y. Z.; Zheng, L. M.; Decurtins, S.; Xin, X. Q. *Chem. Commun.* **2006**, 1745. (d) Yao, H. C.; Li, Y. Z.; Song, Y.; Ma, Y. S.; Zheng, L. M.; Xin, X. Q. *Inorg. Chem.* **2006**, *45*, 59. (e) Lei, C.; Mao, J.-G.; Sun, Y.-Q.; Zeng, H.-Y.; Clearfield, A. *Inorg. Chem.* **2003**, *42*, 6157. (f) Cao, D. K.; Li, Y. Z.; Zheng, L. M. *Inorg. Chem.* **2005**, *44*, 2984.
- (13) (a) Huang, J.; Subbiah, A.; Pyle, D.; Rowland, A.; Smith, B.; Clearfield, A. *Chem. Mater.* **2006**, *18*, 5213. (b) Subbiah, A.; Pyle, D.; Rowland, A.; Narayanan, R. A.; Thiyagarajan, P.; Zon, J.; Clearfield, A. *J. Am. Chem. Soc.* **2005**, *127*, 10826. (c) Song, S. Y.; Ma, J. F.; Yang, J.; Cao, M. H.; Li, K. C. *Inorg. Chem.* **2005**, *44*, 2140. (d) Gao, L. L.; Song, S. Y.; Ma, J. F.; Yang, J. *Cryst. Growth Des.* **2007**, *7*, 895. (e) Song, S. Y.; Ma, J. F.; Yang, J.; Cao, M. H.; Zhang, H.-J.; Wang, H.-S.; Yang, K.-Y. *Inorg. Chem.* **2006**, *45*, 1201.
- (14) (a) Gutschke, S. O. H.; Price, D. J.; Powell, A. K.; Wood, P. T. *Angew. Chem., Int. Ed.* **1999**, *38*, 1088. (b) Zheng, L.-M.; Gao, S.; Yin, P.; Xin, X.-Q. *Inorg. Chem.* **2004**, *43*, 2151.
- (15) (a) Sun, Z.-M.; Prosvirin, A. V.; Zhao, H.-H.; Mao, J.-G.; Dunbar, K. R. *J. Appl. Phys.* **2005**, *97*, 10B305. (b) Palii, A. V.; Ostrovsky, S. M.; Klokishner, S. I.; Reu, O.; Sun, Z.-M.; Prosvirin, A. V.; Zhao, H.-H.; Mao, J.-G.; Dunbar, K. R. *J. Phys. Chem. A* **2006**, *110*, 14003.

- (16) (a) Mateescu, A.; Raptopoulou, C. P.; Terzis, A.; Tangoulis, V.; Salifoglou, A. *Eur. J. Inorg. Chem.* **2006**, 1945. (b) Bauer, S.; Bein, T.; Stock, N. *Inorg. Chem.* **2005**, *44*, 5882. (c) Song, J.-L.; Prosvirin, A. V.; Zhao, H.-H.; Mao, J.-G. *Eur. J. Inorg. Chem.* **2004**, 3706.
- (17) (a) Viviani, R.; Costantino, U.; Nocchetti, M. *J. Mater. Chem.* **2002**, *12*, 3254. (b) Yang, B.-P.; Sun, Z.-M.; Mao, J.-G. *Inorg. Chem. Acta* **2004**, *357*, 1583.

**Table 1.** Summary of Crystal Data and Details of Intensity Collection and Refinement<sup>a</sup>

empirical formula	C <sub>12</sub> H <sub>28</sub> CoN <sub>2</sub> O <sub>16</sub> P <sub>4</sub>
fw	639.17
space group	<i>P</i> 2 <sub>1</sub> / <i>c</i>
<i>a</i> , Å	12.586(3)
<i>b</i> , Å	8.891(1)
<i>c</i> , Å	9.727(3)
β, deg	97.349(4)
<i>V</i> , Å <sup>3</sup>	1079.54(9)
<i>Z</i>	2
<i>D</i> <sub>calcd</sub> , g cm <sup>-3</sup>	1.966
temp, K	293(2)
μ, mm <sup>-1</sup>	1.179
GOF	1.157
R1, wR2 [ <i>I</i> > 2σ( <i>I</i> )]	0.0496, 0.0856
R1, wR2(all data)	0.0611, 0.0899

$$^a R1 = \sum(|F_o| - |F_c|) / \sum |F_o|; wR2 = [\sum w(|F_o| - |F_c|)^2 / \sum wF_o^2]^{1/2}.$$

**Table 2.** Selected Bond Lengths (Å) and Angles (deg) for Compound **1**<sup>a</sup>

Co(1)–O(23)	2.074(2)	P(1)–O(11)	1.514(2)
Co(1)–O(23)#1	2.074(2)	P(1)–O(12)	1.587(2)
Co(1)–O(21)#2	2.121(2)	P(1)–O(13)	1.491(2)
Co(1)–O(21)#3	2.121(2)	P(2)–O(21)	1.504(2)
Co(1)–O(13)	2.158(2)	P(2)–O(23)	1.509(2)
Co(1)–O(13)#1	2.158(2)	P(2)–O(22)	1.574(2)
Hydrogen Bonds			
O(1)⋯O(11)#4	2.605(3)	O(12)⋯O(2)#5	2.619(3)
O(1)–H(1a)⋯O(11)#4	170.4°	O(12)–H(12a)⋯O(2)#5	179.0°
O(23)–Co(1)–O(23)#1	180.0(1)	O(21)#2–Co(1)–O(13)	95.80(8)
O(23)–Co(1)–O(21)#2	87.65(8)	O(21)#3–Co(1)–O(13)	84.20(8)
O(23)#1–Co(1)–O(21)#2	92.35(8)	O(23)–Co(1)–O(13)#1	88.08(8)
O(23)–Co(1)–O(21)#3	92.35(8)	O(23)#1–Co(1)–O(13)#1	91.92(8)
O(23)#1–Co(1)–O(21)#3	87.65(8)	O(21)#2–Co(1)–O(13)#1	84.20(8)
O(21)#2–Co(1)–O(21)#3	180.0(1)	O(21)#3–Co(1)–O(13)#1	95.80(8)
O(23)–Co(1)–O(13)	91.92(8)	O(13)–Co(1)–O(13)#1	180.0(1)
O(23)#1–Co(1)–O(13)	88.08(8)		

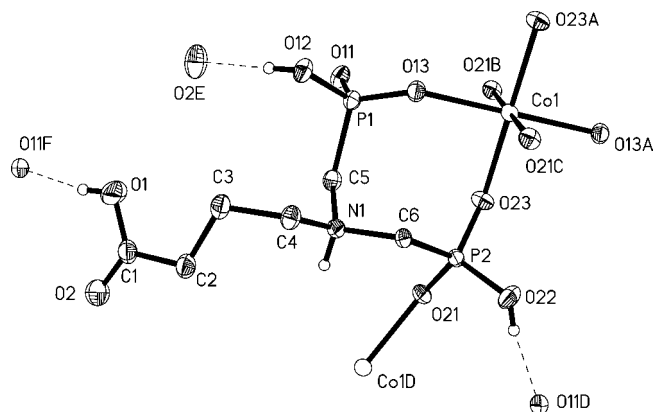
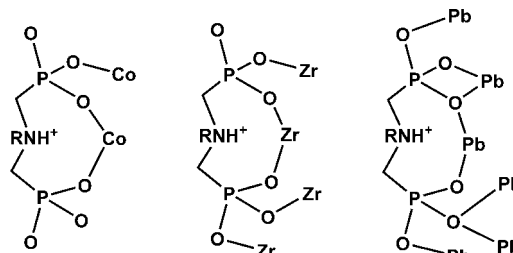
<sup>a</sup> Symmetry transformations used to generate equivalent atoms. #1:  $-x, -y, -z$ . #2:  $-x, y - 1/2, -z - 1/2$ . #3:  $x, -y + 1/2, z + 1/2$ . #4:  $-x + 1, y + 1/2, -z - 1/2$ . #5:  $-x + 1, y - 1/2, -z - 1/2$ .

All non-hydrogen atoms were refined anisotropically. Hydrogen atoms were located at geometrically calculated positions. A summary of crystal data and structure refinement is listed in Table 1. Selected bond distances and angles are given in Table 2. More details on the crystallographic studies are given as Supporting Information.

## Results and Discussion

**Structural Description.** The title compound exhibits a layer architecture that built from CoO<sub>6</sub> octahedra interconnected by phosphonate groups. As shown in Figure 1, the cobalt(II) ion lies on an inversion center and is octahedrally coordinated by six oxygen atoms from six phosphonate groups of four ligands, two of which are in a bidentate chelating mode to form Co–O–P–C–N–C–P–O eight-membered chelating rings, whereas the other two are unidentate. The Co–O bond lengths range from 2.074(2) to 2.158(2) Å, which are comparable to those reported in other cobalt(II) phosphonates.<sup>16</sup> The Co(1)–O(13) bond is slightly longer than the remaining Co–O bonds; hence, the cobalt(II) octahedron is slightly distorted (Table 2).

The carboxylate phosphonate ligand acts as a tridentate chelating and bridging ligand (Scheme 1). It forms an eight-

**Figure 1.** ORTEP drawing showing the coordination environment around the cobalt(II) ion for Co[HO<sub>2</sub>C(CH<sub>2</sub>)<sub>3</sub>NH(CH<sub>2</sub>PO<sub>3</sub>H)<sub>2</sub>]<sub>2</sub>. Hydrogen bonds are represented by dotted lines.**Scheme 1.** Coordination Modes of the H<sub>5</sub>L Ligands in the Title Compound and Its Zr(IV) and Pb(II) Analogues (R = –C<sub>3</sub>H<sub>6</sub>COO(H))

member ring with one Co(1) atom by using two phosphonate groups and also bridges to another metal ion through the coordination of the third phosphonate oxygen atom. One phosphonate group (P(1)O<sub>3</sub>) is unidentate, whereas the other one (P(2)O<sub>3</sub>) is bidentate bridging. Three phosphonate oxygens (O(11), O(12), and O(22)) remain noncoordinated. On the basis of the coordination mode and charge balance as well as P–O and C–O distances, the amine group, O(1) of the carboxylate group, as well as two phosphonate oxygens (O(12) and O(22)) are deduced to be protonated (Table 2); hence, each ligand carries only one negative charge. Such a type of coordination mode is different from those reported in the Zr(IV) and Pb(II) compounds (Scheme 1).<sup>17</sup> In the Zr(IV) compound, the carboxylate–phosphonate ligand is pentadentate, being chelating with one Zr(IV) ion in a bidentate fashion and bridging with three other Zr(IV) ions. In the Pb(II) compound, however, the carboxylate–phosphonate ligand is octadentate, forming a bidentate chelate with two Pb<sup>2+</sup> ions and a bridge to four other Pb<sup>2+</sup> ions; two phosphonate oxygen atoms are bidentate (Scheme 1). In all three compounds, the amine group and the carboxylate group of the ligand remain noncoordinated.

The interconnection of CoO<sub>6</sub> octahedra by bridging phosphonate groups resulted in a <100> 2D square layer with a (4,4)-net topology (Figure 2); the butyric acid moieties of the phosphonate ligands are orientated toward the adjacent layer. The Co–Co separations within a square unit are 6.589(1) Å. The interlayer distances are approximately 12.6 Å, which is close to that of [ZrHF(O<sub>3</sub>PCH<sub>2</sub>)<sub>2</sub>NHC<sub>3</sub>H<sub>6</sub>CO<sub>2</sub>] (13.0 Å) but much smaller than that of Pb<sub>3</sub>[HO<sub>2</sub>–C(CH<sub>2</sub>)<sub>3</sub>NH(CH<sub>2</sub>PO<sub>3</sub>)<sub>2</sub>]<sub>2</sub>·2H<sub>2</sub>O (about 17.0 Å).<sup>17</sup> These 2D

(18) (a) Sheldrick, G. M. *SADABS*; Universität Göttingen: Göttingen, Germany, 1995. (b) Sheldrick, G. M. *SHELXTL*, version 5.1; Bruker-AXS: Madison, WI, 1998.



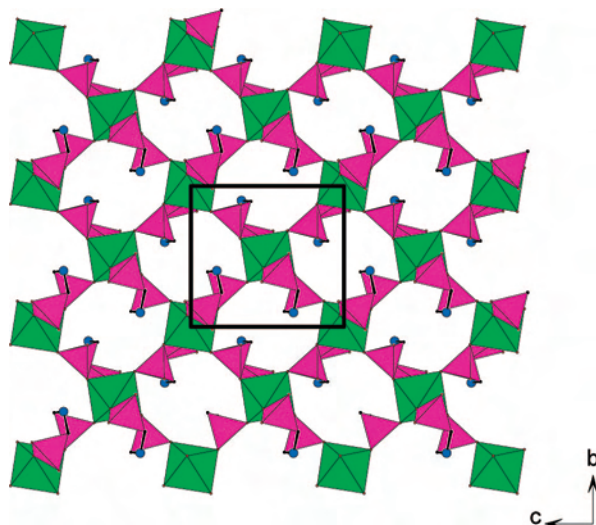


**Figure 2.** A  $\langle 100 \rangle$  layer in  $\text{Co}[\text{HO}_2\text{C}(\text{CH}_2)_3\text{NH}(\text{CH}_2\text{PO}_3\text{H})_2]_2$ . The butyric acid moieties have been omitted for the sake of clarity. The  $\text{CoO}_6$  octahedra and phosphonate tetrahedra are represented in green and pink, respectively. Nitrogen atoms are drawn as blue circles.

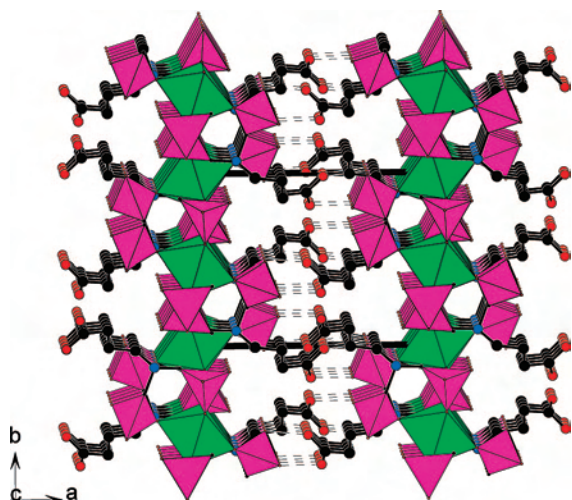


**Figure 3.** View of the crystal structure of  $\text{Co}[\text{HO}_2\text{C}(\text{CH}_2)_3\text{NH}(\text{CH}_2\text{PO}_3\text{H})_2]_2$  down the  $c$  axis. The  $\text{CoO}_6$  octahedra and phosphonate tetrahedra are depicted in green and pink, respectively. Nitrogen atoms are shown as blue circles. Hydrogen bonds are drawn as dotted lines.

layers are further interlinked via hydrogen bonds between the noncoordination carboxylate groups and phosphonate oxygens to form a 3D supramolecular network (Figure 3). The shortest interlayer Co–Co separation is 12.586(1) Å, which is significantly larger than the corresponding distances within the square layer. The noncoordinated carboxylic oxygen atoms (O(1) and O(2)) form two strong hydrogen bonds with noncoordinated phosphonate oxygens (O(11) and O(12)) from a neighboring layer with an O(1)⋯O(11) contact of 2.605(3) Å and an O(2)⋯O(12) separation of 2.619(3) Å (Table 2 and Figure 3). The corresponding hydrogen-bond angles are 170.4 and 179.0°, respectively.

**TGA Study.** TGA curves of the compound show one main step of weight loss. The compound is stable up to 285 °C (see Figure S1, Supporting Information), after which it begins to decompose up to 1000 °C, during which several processes occur: the release of water molecules from the condensation of hydrogen phosphonate groups, the decomposition of the

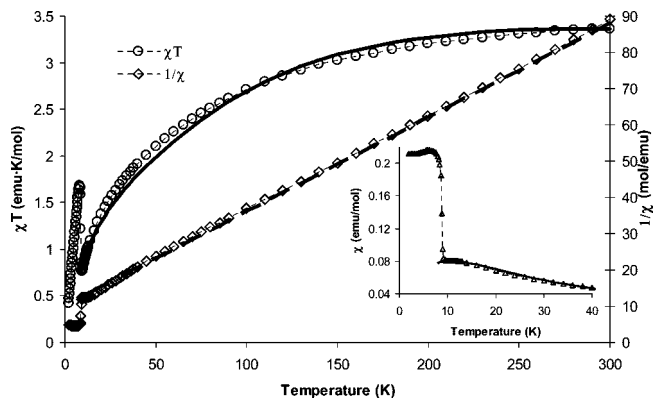


**Figure 4.** Temperature dependence of the  $1/\chi$  ( $\square$ ) and  $\chi T$  product ( $\circ$ ) for  $\text{Co}[\text{HO}_2\text{C}(\text{CH}_2)_3\text{NH}(\text{CH}_2\text{PO}_3\text{H})_2]_2$ . The dashed and solid lines correspond to the best fit to Curie–Weiss law and the spin–orbit coupling model, respectively. Inset: Temperature dependence of  $\chi$ . The solid line corresponds to the best fit to the square lattice model.

carboxylate group, as well as the burning of the other organic groups of the carboxylate–phosphonate ligand. The total weight loss at 1000 °C is 59.9%; the final residuals were not characterized due to a reaction with the  $\text{Al}_2\text{O}_3$  TGA bucket under such high temperatures.

**Infrared Spectroscopy.** The broad IR absorption band at  $3130\text{ cm}^{-1}$  indicates the presence of the  $-\text{OH}$  group in the compound. The intense band in the region  $2200\text{--}2600\text{ cm}^{-1}$  may be due to  $\text{R}_3\text{N}-\text{H}^+$  stretching vibrations. The  $\text{P}=\text{O}$  and  $\text{P}-\text{O}$  stretching and bending bands appear in the region of  $800\text{--}1300\text{ cm}^{-1}$ . There is also a band at  $1660\text{ cm}^{-1}$ , which can be assigned to the antisymmetric  $\text{C}=\text{O}$  stretching vibration mode of the carboxylic group.<sup>17</sup>

**Magnetic Properties.** The temperature dependence of the molar magnetic susceptibility of the title compound at 1 kOe is shown in Figure 4.

The room-temperature  $\chi T$  value of  $3.36\text{ emu}\cdot\text{mol}^{-1}\text{ K}$  ( $5.23\ \mu_{\text{B}}$ ) is much higher than the expected spin-only value for  $S = 3/2$  ( $1.87\text{ emu}\cdot\text{mol}^{-1}\text{ K}$  or  $3.87\ \mu_{\text{B}}$ ), which can be attributed to the spin–orbital interaction of the  $\text{Co}(\text{II})$  ion.<sup>15</sup> However, it is close to the experimental values reported for other  $\text{Co}(\text{II})$  compounds.<sup>19</sup> The  $\chi_{\text{M}}T$  versus  $T$  plot shows that  $\chi_{\text{M}}T$  decreases continuously upon cooling and reaches a minimum of  $0.76\text{ emu K mol}^{-1}$  at 9.4 K. The value then increases to a maximum of  $1.68\text{ emu K mol}^{-1}$  at 8.2 K, followed by a drop toward zero. The upturn of  $\chi_{\text{M}}T$  below 9.4 K suggests uncompensated magnetic moments of the system arising from spin canting of the antiferromagnetically coupled  $\text{Co}(\text{II})$  ions.<sup>20</sup>

The plot of the temperature dependence of magnetic susceptibility is much more informative. Starting from  $0.011\text{ emu}\cdot\text{mol}^{-1}$  at room temperature, the magnetic susceptibility gradually increases to reach a maximum of 0.08 at about 11 K, indicating the presence of antiferromagnetic interactions (Figure 4, inset). The following abrupt jump of the  $\chi$  value

(19) Bourdreaux, E. A.; Mulay, L. N. *Theory and application of molecular magnetism*; Wiley: New York, 1976; p 210.

(20) (a) Lines, M. E. *J. Phys. Chem. Solids* **1970**, *31*, 101. (b) Darriet, J.; Haddad, M. S.; Duesler, E. N.; Hendrickson, D. N. *Inorg. Chem.* **1979**, *18*, 2679.

at 9 K indicates the onset of long-range magnetic ordering, whereupon it finally saturates at 0.21 emu·mol<sup>-1</sup>.

The inverse of susceptibility data obeys the Curie–Weiss law above 10 K, with a Curie constant of 3.86 emu K mol<sup>-1</sup> and a Weiss constant of -42 K (Figure 4). The negative Weiss constant indicates dominant antiferromagnetic interactions and the spin–orbit coupling of the cobalt(II) ion in a slightly distorted octahedral geometry.<sup>19</sup>

A more accurate fit can be obtained by assuming that the <sup>4</sup>T<sub>1g</sub> ground state for high-spin octahedral Co(II) is subject to unquenched spin–orbit coupling as well as zero-field splitting effects.<sup>21</sup> There is no expression, however, that simultaneously accounts for both factors. The Hamiltonian for spin–orbit coupling is written as  $\mathcal{H} = -\lambda LS$ . The  $\chi T$  expression for a mononuclear Co(II) complex in an octahedral environment is provided in eq 1.<sup>21</sup>

$$\chi_{\text{Co}}T = \left[ \frac{7(3-A)^2x}{5} + \frac{12(2+A)^2}{25A} + \left\{ \frac{2(11-2A)^2x}{45} + \frac{176(2+A)^2}{675A} \right\} \exp\left(\frac{-5Ax}{2}\right) + \left\{ \frac{(5+A)^2x}{9} - \frac{20(2+A)^2}{27A} \right\} \exp(-4Ax) \right] / \frac{8x}{3} \left\{ 3 + 2 \times \exp\left(\frac{-5Ax}{2}\right) + \exp(-4Ax) \right\} \quad (1)$$

In this equation,  $x$  equals  $\lambda/k_{\text{B}}T$ , where  $\lambda$  is the spin–orbit coupling parameter, which is -170 cm<sup>-1</sup> for the free ion, and  $A$  is a measure of the crystal-field strength due to the interelectronic repulsions (1.5 for a weak field, 1.0 for a strong field, and 1.32 for a free ion). Due to the magnetic interactions between ions, the expression in eq 1 was corrected using the molecular field approximation (eq 2), where  $\chi$  is the experimental exchange-coupled magnetic susceptibility,<sup>22</sup>  $\chi_{\text{Co}}$  is the magnetic susceptibility in the absence of the exchange field, and  $zJ$  is the exchange parameter; the other symbols have their usual meanings.<sup>23</sup>

$$\chi = \frac{T\chi_{\text{Co}}}{T - \theta} \quad (2)$$

where

$$\theta = \frac{2zJS(S+1)}{3k} \quad (2a)$$

The magnetic data were fitted according to eq 2 in the temperature range of 10–300 K with parameters  $\lambda = -120$  cm<sup>-1</sup> and  $A = 1.5$ , and the results are shown in Figure 4. It should be taken into account that  $\lambda = k\lambda_{\text{freeion}}$ , where  $k$  is a reduction of the spin–orbit coupling due to covalency ( $k = 0.7$ ). For the Co(II) ion in an octahedral environment, an effective “ $S = 1/2$ ” ground state with an effective  $g_{\text{eff}}$  value is expected at low temperatures because of the overall effect

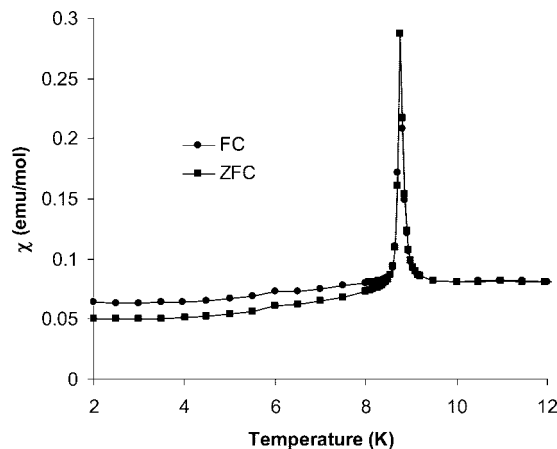


**Figure 5.** Thermal variation of the FC (circle) and ZFC (square) magnetic susceptibilities for Co[HO<sub>2</sub>C(CH<sub>2</sub>)<sub>3</sub>NH(CH<sub>2</sub>PO<sub>3</sub>H)<sub>2</sub>]<sub>2</sub>.

of crystal field and spin–orbit coupling.<sup>23</sup> Assuming  $z = 4$  in a square-planar lattice, the exchange parameter ( $J$ ) was estimated to be -4.2 cm<sup>-1</sup>.

Considering the crystal structure, the low-temperature part of magnetic susceptibility can be alternatively interpreted through eq 3, describing the  $\chi T$  of a 2D Heisenberg quadratic-layer antiferromagnet. This formula, based on spin Hamiltonian  $\mathcal{H} = -2J\sum_{ij}S_iS_j$ , is as follows:<sup>20</sup>

$$\chi T = Ng^2\beta^2 / [4k(1 - 2/x + 2/x^2 - 1.333/x^3 + 0.25/x^4 + 0.4833/x^5 + 0.003797/x^6)] \quad (3)$$

where  $x = kT/J$ ,  $N$  is Avogadro's number,  $\beta$  is the Bohr magneton, and  $k$  is the Boltzmann constant. When the data were fit according to eq 3, an exchange parameter ( $J$ ) of -4.1 cm<sup>-1</sup> and a  $g_{\text{eff}}$  of 5.18 were obtained. The exchange value is comparable to that obtained from eq 2, and  $g_{\text{eff}}$  is typical for Co(II) at low temperatures.<sup>23</sup>

Results of the field-cooled (FC) and zero-field-cooled (ZFC) measurements at 10 Oe exhibit a maximum at  $T_c = 8.75$  K (Figure 5). Above  $T_c$ , the magnetization is reversible and behaves similarly for both FC and ZFC. Below  $T_c$ , however, there is nonreversibility and bifurcation, which is consistent with a spontaneous magnetization below a long-range magnetic phase transition. The application of different magnetic fields in the range of 50–600 Oe showed a strong field dependence of the magnetic susceptibility below  $T_c$ . There is no maximum but is saturation in  $\chi$  under an applied field higher than 200 Oe (See Figure S2, Supporting Information). This field-dependent behavior is indicative of a metamagnetic or spin-flop phase transition exhibited for weakly coupled antiferromagnets.<sup>24,25</sup>

The ac susceptibilities were measured under a 6 Oe alternative field at a frequency range of 1–1000 Hz (some of them are shown in Figure 6). The maximum of  $\chi'$  is observed at  $T_c = 8.75$  K, which is in agreement with the above results and confirms the occurrence of a phase transition. The absence of an out-of-phase signal ( $\chi''$ ) at this

(21) Mabbs, F. E.; Machin, D. J. *Magnetism and Transition Metal Complexes*; Chapman and Hall: London, 1973; p 99.

(22) (a) Wang, X.-Y.; Wei, H.-Y.; Wang, Z.-M.; Chen, Z.-D.; Gao, S. *Inorg. Chem.* **2005**, *44*, 572–583. (b) Zhu, L.-N.; Liang, M.; Wang, Q.-L.; Wang, W.-Z.; Liao, D.-Z.; Jiang, Z.-H.; Yan, S.-P.; Cheng, P. *J. Mol. Struct.* **2003**, *657*, 157–163.

(23) (a) Kahn, O. *Molecular Magnetism*; VCH Publishers: New York, 1993; pp 26. (b) Carlin, R. L. *Magnetochemistry*; Springer-Verlag: Berlin, Heidelberg, 1986.

(24) Price, D. J.; Batten, S. R.; Moubarak, B.; Murray, K. S. *Polyhedron* **2003**, *22*, 2161.

(25) Marvilliers, A.; Parsons, S.; Riviere, E.; Audiere, J.-P.; Kurmoo, M.; Mallah, T. *Eur. J. Inorg. Chem.* **2001**, 1287.

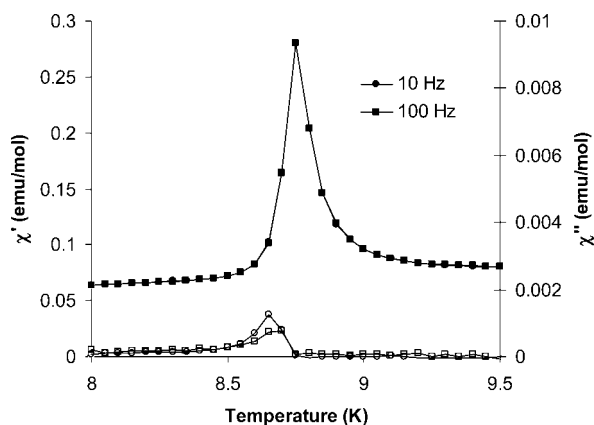


**Figure 6.** The ac susceptibilities of  $\text{Co}[\text{HO}_2\text{C}(\text{CH}_2)_3\text{NH}(\text{CH}_2\text{PO}_3\text{H})_2]_2$  in the presence of a 6 Oe alternating field at 10 and 100 Hz.

temperature points to long-range antiferromagnetic order. However, the imaginary component  $\chi''$  presents an unclear peak at a lower temperature of about 8.6 K, which is a signature of a magnetized state, indicating that a partly canted antiferromagnetic structure takes place below this temperature.<sup>26</sup> No frequency dependence of these transitions is observed.

The magnetic susceptibility is known to vary above  $T_c$  according to the expression<sup>27–30</sup>

$$\chi = \chi_0(1 - T/T_c)^{-\gamma} \quad (4)$$

where  $\gamma$  is the critical exponent and  $\chi_0$  is the critical amplitude above  $T_c$ . The critical exponent  $\gamma$  provides information about the dimensionality and the symmetry of the magnetic lattice undergoing the ordering transition.<sup>27–33</sup> The double logarithmic plots of  $\chi_{\text{FC}}$  and  $\chi'$  as a function of temperature are shown in Figure S3 of the Supporting Information. A fitting of the data according to the power law with  $T_c = 8.75$  K (eq 4) yielded  $\gamma_{\text{FC}} = 0.45$  and  $\gamma_{\text{AC}} = 0.41$ . The obtained critical exponents are smaller than the experimental values reported in 3D ferromagnets ( $\gamma \approx 1.3$ )<sup>27</sup> and the 2D Ising model ( $\gamma \approx 1.75$ )<sup>28</sup> or those predicted by mean field theory ( $\gamma = 1$ ).<sup>31</sup> However, they are close to the values reported for random anisotropy magnets ( $\gamma \approx 0.67$ ),<sup>29</sup>

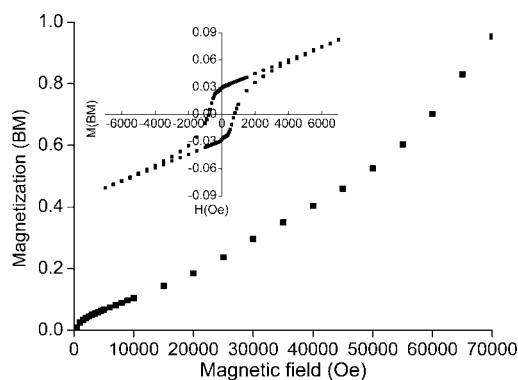


**Figure 7.** Field-dependent magnetization and hysteresis loops (inset) for  $\text{Co}[\text{HO}_2\text{C}(\text{CH}_2)_3\text{NH}(\text{CH}_2\text{PO}_3\text{H})_2]_2$  measured at 1.8 K.

disordered systems ( $\gamma \approx 0.25$ – $0.5$ ),<sup>30</sup> spin-flop transitions ( $\gamma \approx 0.56$ ),<sup>32</sup> and canted systems ( $\gamma \approx 0.35$ – $0.7$ ).<sup>33</sup>

The magnetization measurements at 1.8 K are provided in Figure 7. The initial magnetization increases linearly with the applied field  $H$  and reaches  $0.003 \mu_B$  for  $H = 300$  Oe; after that, it increases slowly up to  $H = 500$  Oe; then, it increases more rapidly with increasing  $H$ . No saturation is observed up to  $H = 7$  T. Clearly, a higher field is required to reach saturation to a ferromagnetic phase. The magnetization curves below  $T_c$  exhibit a hysteresis effect with a coercive field and a small net magnetization  $M_r$ . The coercive field is 800 Oe, and  $M_r = 0.03 \mu_B$  at 1.8 K (Figure 7, inset). The spontaneous magnetization is therefore due to the spin-canting. The estimated canting angle is  $0.75^\circ$ . This angle is calculated according to the equation  $\psi = \sin^{-1}(M_r/M_s)$ , where  $M_r$  is the remnant magnetization and  $M_s = gS$  is the expected saturation magnetization if all the moments are aligned ferromagnetically.<sup>25,34</sup> The spin–orbit coupling and the distortions of octahedral symmetry of the Co(II) ion lead to a lowest-lying Kramers doublet. The effective  $g$  tensor is highly anisotropic, and this usually gives rise to anisotropic exchange interactions as a most probable origin of the weak ferromagnetism.<sup>35</sup>

The field dependence of the magnetization at different temperatures below  $T_c$  and hysteresis in close vicinity of the  $T_c$  display a pronounced sigmoidal shape (Figure 8 and Figure S4, Supporting Information). This is due to the metamagnetic-like behavior (spin-flop or spin-flip). The calculated derivatives  $dM/dH$  also show field-induced spin-reorientational transition (Figure 8, inset) in the range of  $H_c = 100$ – $290$  Oe. The transition field is further proved by the field-dependent ac magnetic susceptibilities (Figure S5, Supporting Information). The obtained value may be accounted for by considering the weak interactions between neighboring planes (dipolar and through hydrogen bonds).<sup>36</sup> The magnitude of the antiferromagnetic interaction between

(26) (a) Huang, Z.-L.; Drillon, M.; Masciocchi, N.; Sironi, A.; Zhao, J.-T.; Rabu, P. P. *Chem. Mater.* **2000**, *12*, 2805–2812. (b) Zeng, M.-H.; Zhang, W.-X.; Sun, X.-Z.; Chen, X.-M. *Angew. Chem., Int. Ed.* **2005**, *44*, 3079–3082.

(27) (a) Binney, J. J.; Dowrick, N. J.; Fisher, A. J.; Newman, M. E. J. *The theory of critical phenomena*; Clarendon: Oxford, U.K., 1992. (b) Bovensiepen, U.; Rudt, C.; Pouloupoulos, P.; Baberscheke, K. *J. Magn. Mater.* **2001**, *231*, 65.

(28) Marcos, M. D.; Gomez-Romero, P.; Amoros, P.; Sapina, F.; Beltran-Porter, D.; Navarro, R.; Rillo, C.; Lera, F. *J. Appl. Phys.* **1990**, *67*, 6998.

(29) Girtu, M. A.; Wynn, C. M.; Zhang, J.; Miller, J. S.; Epstein, A. J. *Phys. Rev. B: Condens. Matter Mater Phys.* **2000**, *61*, 492.

(30) Belayachi, A.; Dormann, J. L.; Nogues, M. *J. Phys.: Condens. Matter* **1998**, *10*, 1599.

(31) Stanley, H. E. *Introduction to phase transitions and critical phenomena*; Clarendon: Oxford, UK, 1971; p 308.

(32) Kawamura, H.; Caille, A.; Plumer, M. L. *Phys. Rev. B: Condens. Matter Mater. Phys.* **1990**, *41*, 4416.

(33) Dormann, J. L.; Belayachi, A.; Nogues, N. *J. Magn. Mater.* **1992**, *104–107*, 239.

(34) Palacio, F.; Andres, M.; Horne, R.; van Duynveldt, A. J. *J. Magn. Mater.* **1986**, *54–57*, 1487.

(35) Sapina, F.; Gomez-Romero, P.; Marcos, M. D.; Amoros, P.; Ibanez, R.; Beltran, D. *Eur. J. Solid State Inorg. Chem.* **1989**, *26*, 603.

(36) (a) Fujiwara, H.; Fujiwara, E.; Nakazawa, Y.; Narymbetov, B. Z.; Kato, K.; Kobayashi, H.; Kobayashi, A.; Tokumoto, M.; Cassoux, P. *J. Am. Chem. Soc.* **2001**, *123*, 306–314. (b) Pereira, C. L. M.; Pedrosa, E. F.; Stumpf, H. O.; Novak, M. A.; Ricard, L.; Ruiz-Garcia, R.; Riviere, E.; Journaux, Y. *Angew. Chem., Int. Ed.* **2004**, *43*, 956–956.



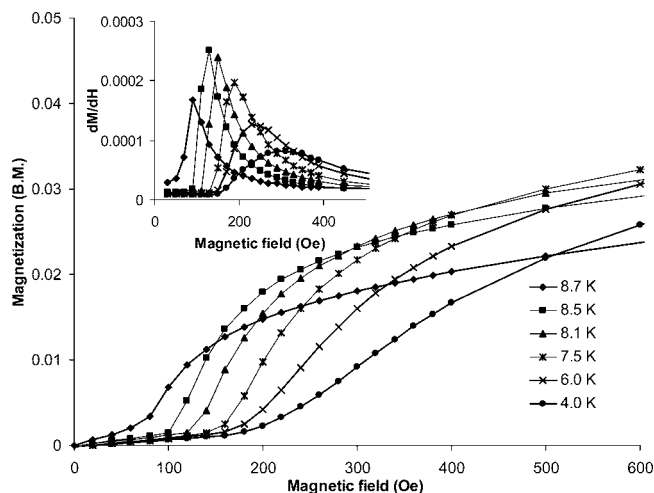


**Figure 8.** Field-dependent magnetization curves measured at different temperatures and plots of  $dM/dH$  vs  $H$  (insets) at different temperatures for Co[HO<sub>2</sub>C(CH<sub>2</sub>)<sub>3</sub>NH(CH<sub>2</sub>PO<sub>3</sub>H)<sub>2</sub>]<sub>2</sub>.

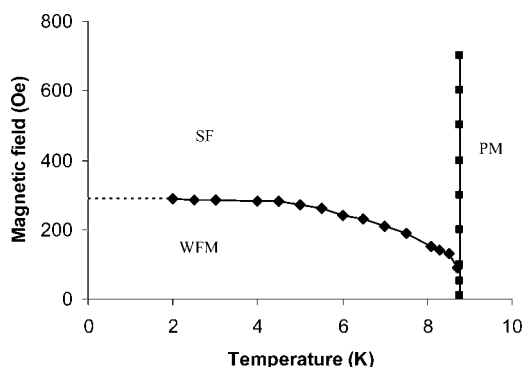


**Figure 9.**  $H(T)$  phase diagram for title compound. WFM = weak ferromagnetic state, SF = metamagnetic-like state (spin-flop or spin-flip), and PM = paramagnetic state. The diamonds and the cubes represent the experimental data obtained from magnetization  $M(H)$  and susceptibility  $\chi(T)$  measurements.

sublattices can be estimated from the exchange energy and magnetic energy at the transition magnetic field  $H_c(0)$  at 0 K:  $-2zJ'S^2 = g\beta SH_c(0)$ . The temperature dependence of the transition field was linearly extrapolated to  $T = 0$  K to obtain  $H_c(0) \approx 290$  Oe. Using this value, the interplane antiferromagnetic exchange was estimated to be  $zJ' = -0.7$  cm<sup>-1</sup>.

According to the aforementioned observations, a magnetic phase diagram of the compound was constructed (Figure 9). The weak ferromagnetic–metamagnetic-like boundary experimental points were obtained from the peaks in  $dM/dH$  curves. These types of phase diagrams are very similar to those reported for the field-induced spin-flop and spin-flip transitions.<sup>38–41</sup> However, in the low-dimensional com-

pounds, it is often the case that the spin-reorientational phenomena (spin-flop or spin-flip) are observed only in one direction.<sup>42</sup> There are some studies showing the simultaneous presence of both of them.<sup>43</sup> Obviously, single-crystal measurements are required for further investigation of magnetic properties of the title compound.

## Conclusions

In summary, a new layered cobalt carboxylate–phosphonate, Co[HO<sub>2</sub>C(CH<sub>2</sub>)<sub>3</sub>NH(CH<sub>2</sub>PO<sub>3</sub>H)<sub>2</sub>]<sub>2</sub>, with a 4,4-connect topology was reported. The compound behaves as a weak ferromagnet below the critical temperature of  $T_c = 8.75$  K. The spin-canting angle is estimated to be 0.75°. The materials also exhibit a metamagnetic-like phase transition at  $H_c(0) \approx 290$  Oe at  $T \rightarrow 0$  K. The cobalt phosphonates are an important class of compounds since the connection of cobalt ions by O–P–O bridges can display a variety of architectures ranging from isolated clusters and 1D chains to 3D networks and display a variety of interesting magnetic properties such as weak ferromagnetism, field-induced magnetic transitions, and single-chain magnet behavior.<sup>4e,14b,15</sup> The title compound is unique in that it displays a novel square layer with large interlayer distances due to the presence of the long amino-carboxylate group. The compound also exhibits interesting magnetic behavior such as weak ferromagnetic interaction below  $T_c$ , spin canting, and a metamagnetic-like phase transition.

**Acknowledgment.** We thank the National Natural Science Foundation of China (No. 20371047, 20521101), NSF of Fujian Province (No. E0610034), and Key project of CAS (No. KJCX2-YW-H01) for financial support. A.V.P. gratefully acknowledges the Department of Energy (award DE-FG02-02ER45999) for the support of this research as well as the National Science Foundation for a grant to purchase the SQUID magnetometer (NSF-9974899). We also thank Prof. Kim Dunbar for her valuable discussion.

**Supporting Information Available:** X-ray crystallographic files in CIF format, TGA curves, and some diagrams showing the magnetic properties for the title compound. This material is available free of charge via the Internet at <http://pubs.acs.org>.

IC701351X

- (37) (a) Feng, M.-L.; Prosvirin, A. V.; Mao, J.-G.; Dunbar, K. R. *Chem.–Eur. J.* **2006**, *12*, 8312. (b) Ma, B.-Q.; Sun, H.-L.; Gao, S.; Su, G. *Chem. Mater.* **2001**, *13*, 1946.  
 (38) Manson, J. L.; Kmety, C. R.; Palacio, F.; Epstein, A. J.; Miller, J. S. *Chem. Mater.* **2001**, *13*, 1068.  
 (39) Wang, X.-Y.; Wei, H.-Y.; Wang, Z.-M.; Chen, Z.-D.; Gao, S. *Inorg. Chem.* **2005**, *44*, 572.  
 (40) Carlin, R. L.; van Duynveldt, A. J. *Acc. Chem. Res.* **1980**, *13*, 231.

(41) de Jongh, L. J.; van Amstel, W. D.; Miedema, A. R. *Physica* **1972**, *58*, 277.

(42) (a) Przychodzen, P.; Lewinski, K.; Balanda, M.; Pelka, R.; Rams, M.; Wasiutynski, T.; Guyard-Duhayon, C.; Sieklucka, B. *Inorg. Chem.* **2004**, *43*, 2967–2974. (b) Greeney, R. E.; Landee, C. P.; Zhang, J. H.; Reiff, W. M. *Phys. Rev. B: Condens. Matter Mater. Phys.* **1989**, *39*, 12200–12214. (c) Wolf, M.; Ruck, K.; Eckert, D.; Krabbes, G.; Müller, K.-H. *J. Magn. Magn. Mater.* **1999**, *196–197*, 569–570.

(43) (a) Wang, X.-Y.; Wang, L.; Wang, Z.-M.; Su, G.; Gao, S. *Chem. Mater.* **2005**, *17*, 6369–6380. (b) Engelfriet, D. W.; Groeneveld, W. L.; Groenendijk, H. A.; Smit, J. J.; Nap, G. M. *Z. Naturforsch., A: Phys. Sci.* **1980**, *35*, 115–128.